Copyright © 2005 Tech Science Press FDMP, vol.1, no.4, pp.301-313, 2005

# Thermal Communication between Two Vertical Systems of Free and Forced Convection via Heat Conduction across a Separating Wall

**M. Mosaad**[1,2], **A. Ben-Nakhi**[2] **and M. H. Al-Hajeri**[2]

**Abstract:** This work deals with the problem of thermal interaction between two fluid media at two different bulk temperatures and separated by a vertical plate. The problem is analyzed by taking into account the heat conduction across the separating plate. The flow configuration considered is one in which the two vertical boundary layers of free and forced convection developed on plate sides are in parallel flow. The dimensionless parameters governing the thermal interaction mechanisms are analytically deduced. The obtained results are presented in graphs to demonstrate the heat transfer characteristics of investigated phenomenon. The work reports a means to estimate the mean conjugate Nusselt number over the entire plate height as a function of controlling parameters.

**keyword:** Free and forced convection, Conduction, Thermal interaction.

## Nomenclature

| | |
|---|---|
| $b$ | plate thickness |
| $g$ | gravitational acceleration |
| $h$ | heat transfer coefficient |
| $k$ | thermal conductivity |
| $L$ | plate height |
| $l$ | scale of free convection layer thickness, Eq. (12) |
| $\overline{Nu}$ | mean conjugate Nusselt number, $=\overline{q}L/(k\Delta t)$ |
| $Nu_{xc}$ | local Nusselt number of cold forced convection side, $=h_{xc}x/k_c$ |
| $Nu_{xh}$ | local Nusselt number of hot free convection side, $=h_{xh}x/k_h$ |
| $Pr$ | Prandtl number, $= \nu / \alpha$ |
| $\overline{q}$ | mean heat flux over entire wall height |
| $Ra$ | modified Rayleigh number, Eq. (12) |
| $Ra_x$ | local Rayleigh number based on ($t_{h\infty}$ - $t_{wh}$(x)) |
| $Re_L$ | Reynolds number, $= u_\infty L/\nu$ |
| $t$ | temperature |
| $t_{h\infty}$ | free hot fluid temperature |
| $t_{c\infty}$ | free cold fluid temperature |
| $\Delta t$ | total temperature drop across two fluid media, $= (t_{h\infty} - t_{c\infty})$ |
| $u, v$ | velocity components in $x$- and $y$-directions, respectively |
| $U, V$ | dimensionless velocity components in $x$- and $y$-directions, respectively |
| $x, y$ | vertical and horizontal coordinates, cf., Fig. 1 |
| $X, Y$ | dimensionless vertical and horizontal coordinates |

### Greek letters

| | |
|---|---|
| $\Delta$ | dimensionless thickness of forced convection velocity layer , Eq. (7) |
| $\Delta_t$ | dimensionless thickness of forced convection thermal layer |
| $\alpha$ | thermal diffusivity |
| $\beta$ | thermal expansion coefficient |
| $\beta_0, \beta_1$ | variable coefficients, Eq. (30) |
| $\delta$ | thickness of forced convection velocity layer |
| $\sigma$ | thickness ratio of thermal to velocity layer, $=\Delta_t/\Delta$ |
| $\gamma_0, \gamma_1$ | variable coefficients, Eq. (30) |
| $\eta$ | inverse Oseen function, $= 1/\lambda$ |
| $\lambda$ | Oseen function |
| $\nu$ | kinematic viscosity. |
| $\theta$ | dimensionless temperature, Eq. (3) |
| $\omega$ | dimensionless wall parameter, Eq. (25) |
| $\psi$ | dimensionless function, Eq. (27) |
| $\zeta$ | dimensionless conjugation parameter, Eq. (25) |

### Subscripts

| | |
|---|---|
| $c$ | cold fluid |
| h | hot fluid |
| $x$ | local value |
| $w$ | wall |
| $wc$ | wall-fluid interface of cold side |
| $wh$ | wall-fluid interface of hot side. |

[1] on leave from Mansoura University of Egypt, correspondence to whom be sent, P.O. Box 64268, Faculty of Technological Studies, Suaikh 70453, Kuwait, e.-mail: Mosaad@paaet.edu.ku

[2] Faculty of Technological Studies, Mech. Power & Refrigeration Dept., Kuwait

## 1 Introduction

Throughout the past three decades many researchers have concerned with the thermal interaction phenomenon between two convection systems. This is reflected in many recent studies treating various types of conjugate convection problems. Among those types is the problem of two convection systems separated by a vertical plate, which may be encountered in many engineering applications such as nuclear reactor cooling, air conditioning systems, heat exchangers, and thermal buildings insulation. However, modeling such a conjugate convection problem is complicated, because it is necessary to solve simultaneously the governing equations of two convection modes and the wall heat conduction equation without any prescription for the interfacial temperature or heat flux at plate sides.

Conjugate convection problems may be classified based on the type of involved convection modes into three categories: (a) two forced convection systems, (b) two natural convection systems, and (c) a forced convection system and a free convection system. Analogous classification can be given for the conjugation between mixed convection and free or forced convection. The type (a) of two forced convection systems was initially treated by Mori *et. al*. (1980), who proved based on their numerical results that the heat conduction in the separating wall relaxes the thermal interaction between the two convection systems. However, the analysis of this problem type is less complicated than the other two types (b) & (c) of free convection part. This is because the energy and momentum equations of the forced convection layer can be solved separately, while those of the free convection layer have to be solved simultaneously.

With respect to the thermal communication between two natural convection systems, many studies have recently been published. The first work was done by Lock and Ko (1973), who used the similarity transformation technique with the finite difference method to solve the problem by taking into account the transversal heat conduction in the separating wall. They stated that the wall heat conduction has a remarkable effect on the thermal interaction between the two convection systems. Later, Viskanta and Lankford (1981) analyzed the same problem by using the superposition technique, and derived results that were similar to those obtained by Lock and Ko. However, in a subsequent study, Sakakibara and Amaya (1992) mentioned that the superposition technique is not adequate to treat such a conjugate problem because of the nonlinearity in the fundamental equations of free convection. Perhaps the most important contribution in this research point could be attributed to Bejan and Anderson (1980-1983, who used the Oseen analytic technique (modified originally by Gill 1966), to treat three cases of this thermal conjugation type between: $(a)$ two newtonian fluids, $(b)$ two porous fluids, and $(c)$ a porous fluid and a newtonian fluid. In their models, the separating wall was assumed either as a partition with negligible thermal resistance or with finite thickness of considerable heat conduction resistance only in the transversal direction. Following Bejan and Anderson, the technique of Oseen has been used in a number of subsequent studies.

Regarding the thermal interaction between free convection system and forced convection system, a few studies have recently been published. The first work was done by Sparrow and Faghri (1980), who treated numerically the coupled heat transfer between upward fully developed forced flow inside a vertical circular tube and upwards-induced ambient natural convection, with neglecting the tube wall resistance.

In a more recent study, Mosaad and Ben-Nakhi (2003) developed an analytical model for the conjugate heat transfer between two vertical free and forced convection layers, in parallel flow on the opposite sides of a vertical wall. Following Bejan and Anderson (1980), the separating wall was assumed as a partition without thermal resistance. So, the problem was simplified into two adjacent free and convection layers, whose solutions were derived from using the same set of boundary conditions at the common fluid-fluid interface. Despite this extreme simplification, the main advantage of such an analytical approach is that the parametric dependence of the interactive heat transfer mechanisms is considerably more visible than in a numerical solution. However, to achieve better modeling for the physical reality of the investigated phenomenon, the wall heat conduction effect, neglected in our previous simple model, has been considered in the present approach.

## 2 Analysis

The physical model and coordinate systems used are sketched in Fig. 1. Two semi-infinite fluid media at two different free temperatures communicate thermally

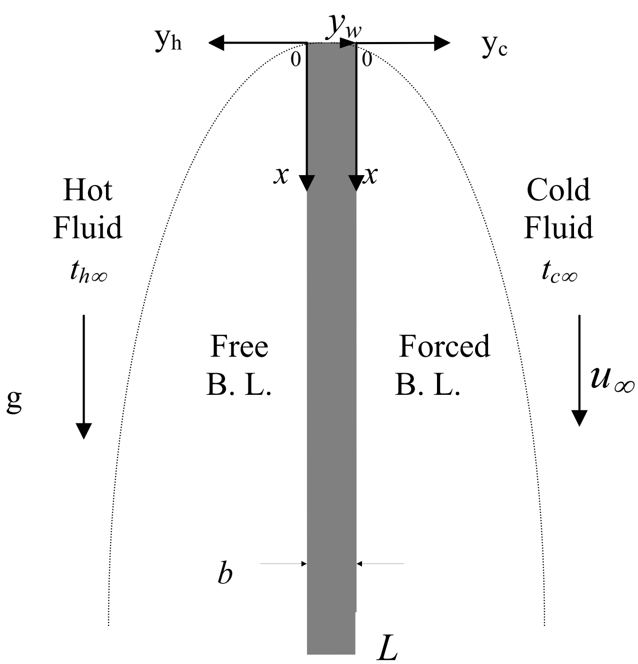


**Figure 1** : Physical model

across a vertical separating plate of height $L$ and thickness $b$. The cold fluid is at free temperature $t_{c\infty}$ and flows downwards with free velocity $u_\infty$along one of two vertical plate sides. The hot fluid on the opposite side is stagnant and at temperature $t_{h\infty} >> t_{c\infty}$. As a result of heat transfer from the hot to the cold medium, free convection layer is induced on the hot plate side with downward flow.

In such a situation, the development of two thermal boundary layers on the opposite plate surfaces depends on the interfacial temperature on both sides, which cannot be prescribed in the analysis, rather, determined from the conjugate solution which requires the coupling between the fundamental equations of two convection layers and plate heat conduction. Thus, the stated problem seems to be complicated.

Therefore, the following simplifications of boundary layer theory are introduced in order to simplify the analysis of two convection layers:

1. Steady, laminar, two-dimensional flow in both layers
2. Negligible axial conduction and viscous dissipation in both layers
3. Zero pressure gradients outside two layers
4. Constant physical properties with applying Boussinesq approximation on the free layer
5. Hot stagnant fluid of $Pr_h >> 1$, and cold forced-flow fluid of $Pr_c$ = O(1)

Moreover, the heat conduction in the plate is assumed only in the transverse direction. Just as a brief conclusion of the analysis, presented in next subsections, the free convection layer has been analyzed by the Oseen analytical technique, while the forced convection layer has been analyzed by the integral technique. Then, the two analyses have been coupled with the plate heat conduction solution to yield the conjugate solution. For the sake of clarity in presentation, subscripts "c, h, w" have been used to sign to the cold fluid, the hot fluid and the wall, respectively.

### *2.1 Forced convection*

The integral momentum and energy equations of forced boundary layer can be expressed in the dimensionless forms:

$$\frac{d}{dX}\int_0^{\Delta} U_c(U_c-1)dY_c = -\left.\frac{\partial U_c}{\partial Y_c}\right|_{Y_c=0} \tag{1}$$

$$\frac{d}{dX}\int_0^{\Delta_t} U_c(\theta_c+1/2)dY_c = -\left.\frac{1}{Pr_c}\frac{\partial \theta_c}{\partial Y_c}\right|_{Y_c=0} \tag{2}$$

The dimensionless variables introduced above are defined as

$$\begin{aligned} &X=\frac{x}{L}, \quad Y_c=\frac{y_c}{L}Re_L^{1/2},\\ &\Delta=\frac{\delta}{L}Re_L^{1/2}, \quad \Delta_t=\frac{\delta_t}{L}Re_L^{1/2},\\ &U_c=\frac{u_c}{u_\infty}, \quad \theta_c=(t_c-0.5(t_{h\infty}+t_{c\infty}))/\Delta t \end{aligned} \tag{3}$$

where $X$ and $Y_c$ are the dimensionless coordinates on the cold side, $\Delta$ and $\Delta_t$ are the dimensionless local thickness of velocity and thermal layers, and $U_c$ and $\theta_c$ are the dimensionless local velocity and temperature, respectively. The symbol $\Delta t(=t_{h\infty}-t_{c\infty})$ denotes the total temperature drop across the two media, $Re$ $(=u_\infty L/\nu_c)$ is Reynolds number, and $Pr_c$ is Prandtl number of the cold fluid.

The appropriate velocity and temperature boundary conditions are

$$at \quad Y_c = 0; \quad U_c = 0, \quad \partial^2 U_c/\partial Y_c^2 = 0, \quad \theta_c = \theta_{wc}(X), \quad \partial^2\theta_c/\partial Y_c^2 = 0$$

$$at \quad Y_c = \Delta; U_c = 1, \quad \partial U_c/\partial Y_c = 0, \quad Y_c = \Delta_t; \quad \theta_c = -1/2, \quad \partial\theta_c/\partial Y_c = 0. \tag{4}$$

where $\theta_{wc} = (t_{wc} - 0.5(t_{h\infty} + t_{c\infty}))/\Delta t$ is the dimensionless local temperature of plate side facing the cold fluid, which is a function of $X$-coordinate to be determined.

The cubic velocity and temperature profiles satisfying boundary conditions (4) are, respectively,

$$U_c = \frac{3}{2}\left(\frac{Y_c}{\Delta}\right) - \frac{1}{2}\left(\frac{Y_c}{\Delta}\right)^3; \quad 0 \le Y_c \le \Delta \tag{5}$$

$$\frac{(\theta_c + 1/2)}{(\theta_{wc} + 1/2)} = 1 - \frac{3}{2}\left(\frac{Y_c}{\Delta_t}\right) + \frac{1}{2}\left(\frac{Y_c}{\Delta_t}\right)^3; \quad 0 \le Y_c \le \Delta_t \tag{6}$$

Solving Eqs. (1) and (2) for above velocity and temperature profiles yields, respectively,

$$\Delta = \sqrt{280X/13} \tag{7}$$

$$\frac{d}{dX}\left[\Delta_t(\theta_{wc} + 1/2)\right] = \frac{10(\theta_{wc} + 1/2)}{\{(\sigma - \sigma^3/14)Pr_c\Delta_t\}} \approx \frac{10(\theta_{wc} + 1/2)}{\{\sigma Pr_c\Delta_t\}} \tag{8}$$

where $\sigma$ (=$\Delta_t/\Delta$) is the thickness ratio of thermal to velocity layer.

### 2.2 Free convection

The mass, momentum and energy equations of the free convection layer may be written, respectively, in the dimensionless forms:

$$\frac{\partial U_h}{\partial X} + \frac{\partial V_h}{\partial Y_h} = 0 \tag{9}$$

$$\frac{\partial \theta_h}{\partial Y_h} = -\frac{\partial^3 U_h}{\partial Y_h^3} \tag{10}$$

$$U_h\frac{\partial \theta_h}{\partial X} + V_h\frac{\partial \theta_h}{\partial Y_h} = \frac{\partial^2 \theta_h}{\partial Y^2} \tag{11}$$

The dimensionless variables and parameters introduced above are defined as

$$Y_h = y_h/l, \quad U_h = u/(\alpha_h L/l^2), \quad V_h = v_h/(\alpha_h/l), \quad Pr_h = \upsilon_h/\alpha_h, \quad l = LRa^{-1/4}, \quad Ra = g\beta_h L^3\Delta t/(\upsilon_h\alpha_h), \quad \theta_h = (t_h - 0.5(t_{h\infty} + t_{c\infty}))/\Delta t \tag{12}$$

In above, $U_h$ and $V_h$ are the velocity components in the $X-$ and $Y_h-$ direction, respectively, $Ra$ is the modified Rayleigh number based on total wall height $L$ and total temperature drop $\Delta t$ across the two media. The variables $\beta_h$, $\upsilon_h$, $\alpha_h$ *and* $\Pr_h$ are, respectively, the thermal expansion coefficient, kinematic viscosity, thermal diffusivity and Prandtl number of the hot fluid.

The scale of free layer thickness;introduced *by* $l = LRa^{-1/4}$, satisfies the requirement of boundary layer theory that the ratio $l/L << 1$. Equation (10) is derived by eliminating the pressure gradients between the x- and y-momentum equations; after cross differentiating and subtracting those two equations. Further, In this simplified momentum equation, the inertia terms are neglected relative to the body force and the viscous shear force. This scaling is valid for Prandtl number >>1 (Baehr (1998)).

The appropriate velocity and temperature boundary conditions are:

$$at \quad Y_h = 0, \quad U_h = V_h = 0 \text{ and } \theta_h = \theta_{wh}(X) \tag{13}$$

$$\text{as} \quad Y_h \to \infty, \quad U_h = 0, \quad \theta_h = 1/2. \tag{14}$$

where $\theta_{wh} = (t_{wh} - 0.5(t_{h\infty} + t_{c\infty}))/\Delta t$ is the dimensionless local temperature of the wall side facing the hot fluid, which is a function of $X$-variable to be determined.

Following previous studies (e.g., Poulikakos (1986) and Mosaad (1999) among others), the modified Oseen technique of Gill can be employed to solve Eqs. (9)-(11) subject to above boundary conditions. In this technique, the horizontal velocity component $V_h$ and temperature gradient $(\partial\theta_h/\partial X)$ in energy Eq. (11) are considered as functions of $Y_h$-coordinate only. Consequently, this equation can be coupled with momentum Eq. (10) to yield an ordinary differential equation that can be solved analytically to yield the following velocity and temperature profiles:

$$U_h = (1/2 - \theta_{wh})\frac{(e^{-\lambda Y_h}\sin\lambda Y_h)}{2\lambda^2} \tag{15}$$

$$\theta_h = 1/2 + (\theta_{wh} - 1/2)e^{-\lambda Y_h} \cos \lambda Y_h \tag{16}$$

Subject to Eqs. (13) & (14), examining above velocity and temperature profiles reveals that the unknown Oseen function $\lambda$ $(X)$ plays the role of the inverse of free layer thickness. Therefore, $\lambda$ has to assume positive values only.

Integrating energy equation (11) across the boundary layer from $Y_h = 0$ to $\infty$ by using the above $U_h$and $\theta_h$ profiles yields:

$$\frac{d}{dX}\left[\frac{(1/2-\theta_{wh})^2}{16\lambda^3}\right] = \lambda(1/2-\theta_{wh}) \tag{17}$$

For more detail on Oseen procedure, the reader can refer to Anderson and Bejan (1980) among other sources. Here it is important to state that above ($\theta_{wh}$, $\lambda$ )-relation and ($\theta_{wc}$, $\Delta_t$ )-relation (8) involve four unknown parameters: $\theta_{wh}$, $\lambda$, $\theta_{wc}$ and $\Delta_t$.

### 2.3 Plate heat conduction

The height of the solid plate is assumed much greater than its thickness, *i.e.* *L/b*<<1. Thus, the longitudinal heat conduction in the plate may be neglected relative to the transverse conduction. Thus, the heat conduction in the plate can be modeled by

$$\frac{\partial^2\theta_w}{\partial y_w^2} = 0; \tag{18}$$

subject to the boundary conditions:

$$\theta_w = \theta_{wh}(X) \quad at \quad Y_w = 0, \tag{19}$$

$$\theta_w = \theta_{wc}(X) \quad at \quad Y_w = 1. \tag{20}$$

The dimensionless variables introduced above are defined,

$$Y_w = y_w/b, \quad \theta_w = (t_w - 0.5(t_{h\infty} + t_{c\infty}))/(t_{h\infty} - t_{c\infty}) \tag{21}$$

Solving Eq. (18) according to boundary conditions (19) & (20) gives

$$\theta_w = \quad \theta_{wh} - (\theta_{wh} - \theta_{wc})Y_w \tag{22}$$

### 2.4 Interfacial conditions

At a certain vertical position ($x$), the continuity of heat flux and temperature at plate sides reads:

$$k_h \left.\frac{\partial t_h}{\partial y_h}\right|_{y_h=0} = -k_c \left.\frac{\partial t_c}{\partial y_c}\right|_{y_c=0} = -k_w \left.\frac{\partial t_w}{\partial y_w}\right|_{y_w=0} \tag{23}$$

Above relation can be expressed in the dimensionless form:

$$\zeta \left.\frac{\partial\theta_h}{\partial Y_h}\right|_{Y_h=0} = -\left.\frac{\partial\theta_c}{\partial Y_c}\right|_{Y_c=0} = \frac{\theta_{wh}-\theta_{wc}}{\omega} \tag{24}$$

The two dimensionless parameters appeared above are defined,

$$\omega = \frac{bk_c}{Lk_w} Re_L^{1/2} \quad \text{and} \quad \zeta = \frac{k_h Ra_L^{1/4}}{k_c Re_L^{1/2}} \tag{25}$$

$\omega-$parameter relates plate thermal resistance to forced convection resistance, and $\zeta-$parameter represents the thermal resistance ratio of forced and free convection layers.

Inserting Eqs. (6) and (16) into (24), this yields after variables separation process the two relations:

$$\theta_{wc} + 1/2 = \frac{2\zeta\Delta_t}{3\psi} \tag{26}$$

$$\theta_{wh} - 1/2 = -\frac{\eta}{\psi} \tag{27}$$

wherein: $\psi = [\eta + \zeta(\omega + \frac{2}{3}\Delta_t)]$; $\quad \eta = 1/\lambda$.

Substituting Eq. (26) into Eq. (8), and Eq. (27) into Eq. (17) yields; after performing differentiation and variables separation, the following two differential equations:

$$\frac{d\Delta_t}{dX} = \frac{\gamma_0 + \gamma_1\beta_0}{1-\gamma_1\beta_1} \tag{28}$$

$$\frac{d\eta}{dX} = \frac{\beta_0 + \gamma_0\beta_1}{1-\gamma_1\beta_1} \tag{29}$$

The variable coefficients in Eqs. (28) and (29) are defined as

$$\gamma_0 = \frac{15\psi}{\emptyset pr_c(3\psi - \zeta\Delta_t)\Delta_t}, \quad \gamma_1 = \frac{3\Delta_t}{2(3\psi-\zeta\Delta_t)},$$
$$\beta_0 = \frac{16\psi^2}{(5\psi-2\eta)\eta^4}, \quad \beta_1 = \frac{4\zeta\eta}{3(5\psi-2\eta)}. \tag{30}$$

So far, Eqs. (26)-(28) are considered the more important results of the analysis, because their solutions will provide the $X$-distributions of $\Delta_t$, $\eta$, $\theta_{wh}$ *and* $\theta_{wc}$ along the wall as functions of $\zeta$, $\omega$ and $\mathrm{Pr}_c$.

The local Nusselt number of free convection side, $Nu_{xh} = (h_{xh}x/k_h)$, can be calculated by

$$\frac{Nu_{xh}}{Ra_x^{1/4}} = \frac{X^{0.5}}{(0.5-\theta_{wh})}\frac{\partial\theta_c}{\partial Y_h}\bigg|_{Y_h=0} \tag{31}$$

Similarly, the local Nusselt number of forced convection side, $Nu_{xc} = (h_{xc}x/k_c)$, is defined as

$$\frac{Nu_{xc}}{Re_x^{1/2}} = -\frac{X^{0.5}}{(\theta_{wc}+0.5)}\frac{\partial\theta_c}{\partial Y_c}\bigg|_{Y_c=0} \tag{32}$$

However, the work should, most importantly, provide the average wall heat flux over the entire plate height, which is defined as

$$\overline{q} = \frac{k_h}{L}\int_0^1 \frac{\partial t_h}{\partial y_h}\bigg|_{y_h=0} dX = -\frac{k_c}{L}\int_0^1 \frac{\partial t_c}{\partial y_c}\bigg|_{y_c=0} dX \tag{33}$$

The above relation can be expressed in a dimensionless form related to the forced convection side, in terms of the mean conjugate Nusselt number $\overline{Nu} = \overline{q}L/(k_c\Delta t)$, as

$$\frac{\overline{Nu}}{Re_L^{1/2}Pr_c^{1/3}} = \frac{-1}{Pr_c^{1/3}}\int_0^1 \frac{\partial\theta_c}{\partial Y_c}\bigg|_{Y_c=0} dX \tag{34}$$

Or related to the free convection side, in terms of $\overline{Nu} = \overline{q}L/(k_h\Delta t)$, as

$$\frac{\overline{Nu}}{Ra^{1/4}} = \int_0^1 \frac{\partial\theta_h}{\partial Y_h}\bigg|_{Y_h=0} dX \tag{35}$$

## 3 Solution and results discussion

Equations (27) and (28) are implicit and dependent differential equations involving two unknown parameters $\Delta_t$ and $\eta$. Therefore, they have to be solved simultaneously to determine the $X$-distributions of these two parameters over the entire wall height as functions of $\zeta$, $\omega$ and $pr_c$. However, a simultaneous numerical integration of these two equations requires that the initial boundary values of $\Delta_t$ and $\eta$ at the start point of boundary layer at $X$=0 have to be known. Investigating Eqs. (15) and (16) proves that the inverse Oseen function $\eta$ (=1/$\lambda$) plays the role of the dimensionless thickness of free convection layer. Based on Fig. 1, $\Delta_t$ and $\eta$ have to assume zero values at $X$=0. However, the singularity problem in solving Eq. (27) & (28) for $\eta$=0 and $\Delta$=0 requires using another appropriate initial values to overcome this problem.

Solving Eqs. (27) & (28) for the limits: $\Delta_t \rightarrow 0$ and $\eta \rightarrow 0$ as $X \rightarrow 0$, yields, respectively,

$$\Delta_{t_0} = 0.9756\Delta_0/pr_c^{1/3} \quad \text{and} \quad \eta_0 = (64X_0/3)^{1/4} \tag{36}$$

where $X_o$ is very small value of $X$ and $\Delta_o$ is calculated by Eq. (7) for $X = X_o$.

The fourth-order Runge-Kutta integral procedure was employed to solve Eqs (27) and (28) numerically using the above initial values $\Delta_o$ and $\eta_0$. It was found that the solution with $X_o$= 0.00001 and step size$\Delta X$= *0.005* gives stable and accurate results. Numerical results have been obtained for wide ranges of $\zeta$ , $\omega$ and $Pr_c$.

At first, the results obtained for the thin-wall case are discussed. For this case of $\omega \rightarrow 0$, Eqs. (26) & (27) yields$\theta_{wc} \rightarrow -1/2$ & $\theta_{wh} \rightarrow -1/2$ as $\zeta \rightarrow 0$, respectively. Consequently, Eq. (6) shows that $\theta_c \rightarrow -1/2$. This means that on this $\zeta \rightarrow 0$ limit, the temperature in the plate and the forced convection layer becomes uniform and takes the low extreme value –1/2 of the cold medium temperature. So, on this limit, the two-fluid problem collapses to the classical one-fluid problem of free convection on an isothermal vertical surface. The relevant analytical solution of this limit, derived in appendix (I), yields the mean Nusselt number result:

$$\overline{Nu}/Ra^{1/4} = 0.621 \tag{37}$$

This result agrees within 2.5% with the exact result of free convection on isothermal vertical surfaces, obtained by a similarity solution for $Pr_h \rightarrow >> 1$ (Baehr (1998)).

On the opposite limit: $\zeta \rightarrow \infty$, Eqs. (26) & (27) for $\omega \rightarrow 0$ yield $\theta_{wc} \rightarrow 1/2$ and $\theta_{wh} \rightarrow 1/2$, respectively. Hence, Eq. (16) shows that $\theta_h \rightarrow 1/2$. This implies that the temperature in the wall and free convection layer region assumes the extreme value 1/2 of the hot side temperature. This means making the free convection layer on the hot side to disappear and, so reducing the conjugate problem to the classical problem of forced convection on an isothermal vertical surface. The related solution can be deduced by reworking the analysis part of forced convection for $\theta_{wh}$= 1/2, as described in appendix I. This solution yields the result:

$$\overline{Nu}/(Re_L^{1/2}Pr_c^{1/3}) = 0.664 \quad (38)$$

This result is the same known similarity solution of forced convection on an isothermal surface, recommended for $0.6 \le Pr_c \le 10$ (Sparrow and Gregg (1965)). The above two asymptotic results (37) & (38) of thin-wall case prove the validity of present analytical approach. Here, it is important to point out that in the preliminary tests of employed numerical technique; these two exact results were used as a reference to adjust the accuracy of the numerical solution as well as to ensure its reliability.

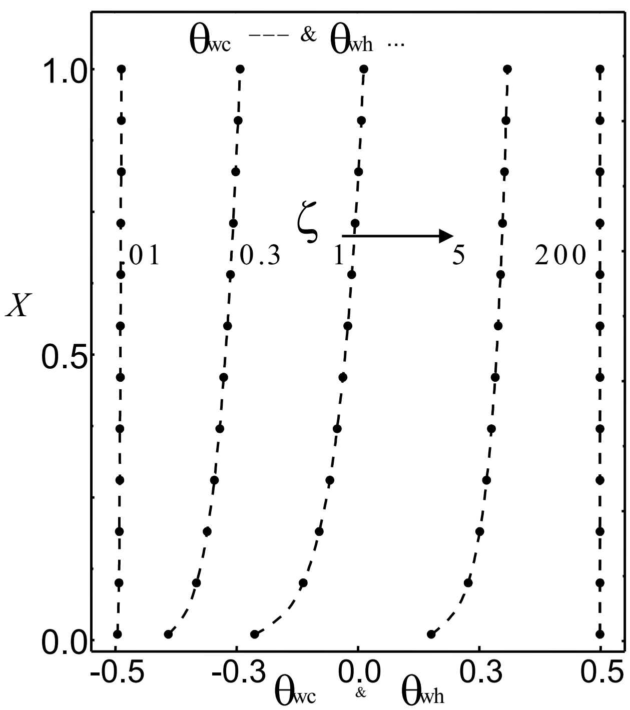


**Figure 2** : Interfacial temperature distribution at interface sides for various $\zeta$ at $\omega$=0.

Numerically obtained results for the thin-wall case of $\omega$=0 are displayed in Fig. 2, where the distribution of temperature at both interface sides $\theta_{wh}$and $\theta_{wc}$ are plotted for various values of $\zeta$. In this case, the separating wall acts as a partition of zero thermal resistance. Therefore, the two predicted profiles of $\theta_{wh}$and $\theta_{wc}$are identical and represented by a common curve in Fig.2. It was also found that for $\zeta \to 0$ or $\zeta \to \infty$, both $\theta_{wh}$and $\theta_{wc}$ take nearly a uniform value over the entire wall height. This

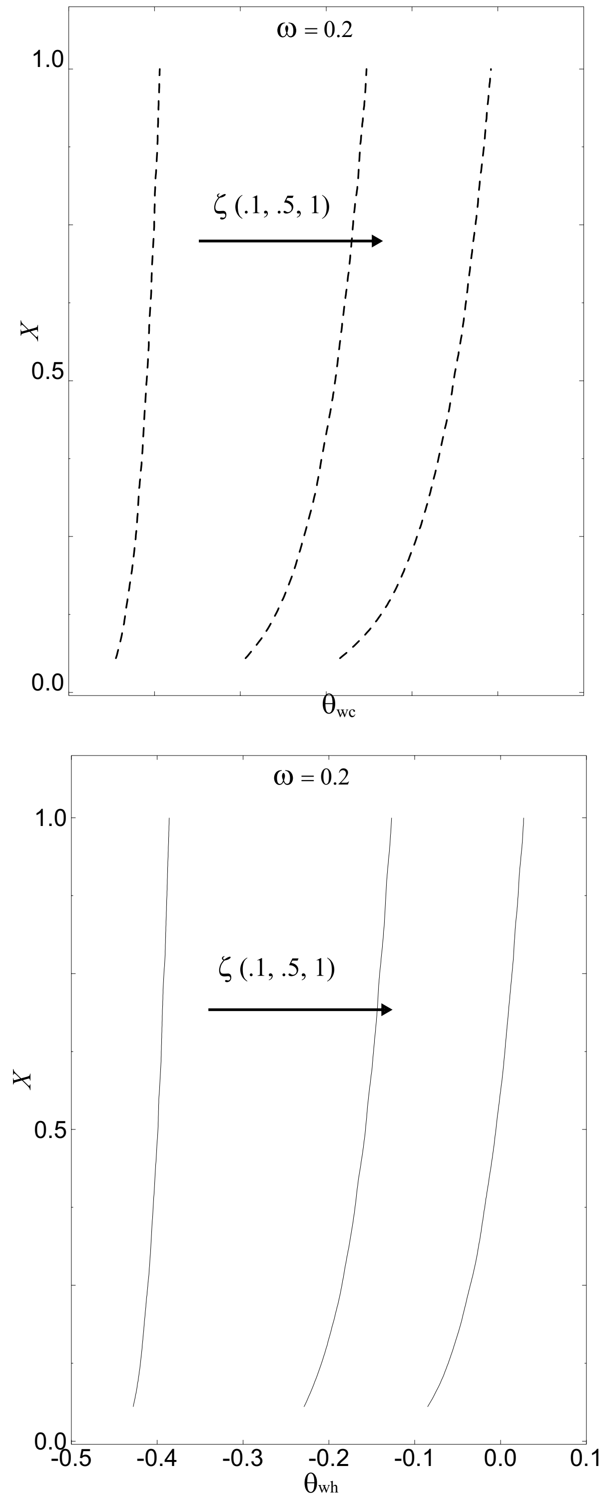


**Figure 3** : Interfacial temperature distribution at both plate sides for various $\zeta$, at $\omega$=2.

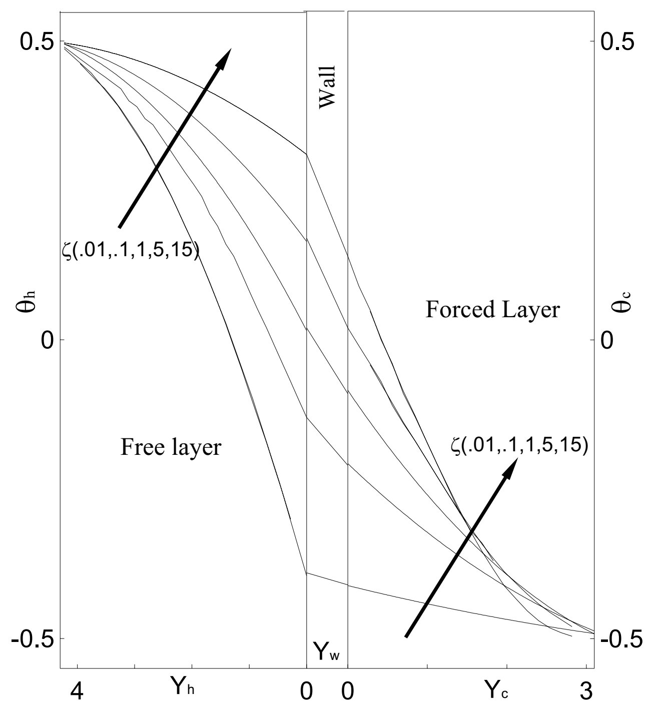


**Figure 4** : Temperature profile across two convection layers and solid plate for various $\zeta$ at $X$=0.5, for $\omega$=0.5 & $Pr_c$ =1.

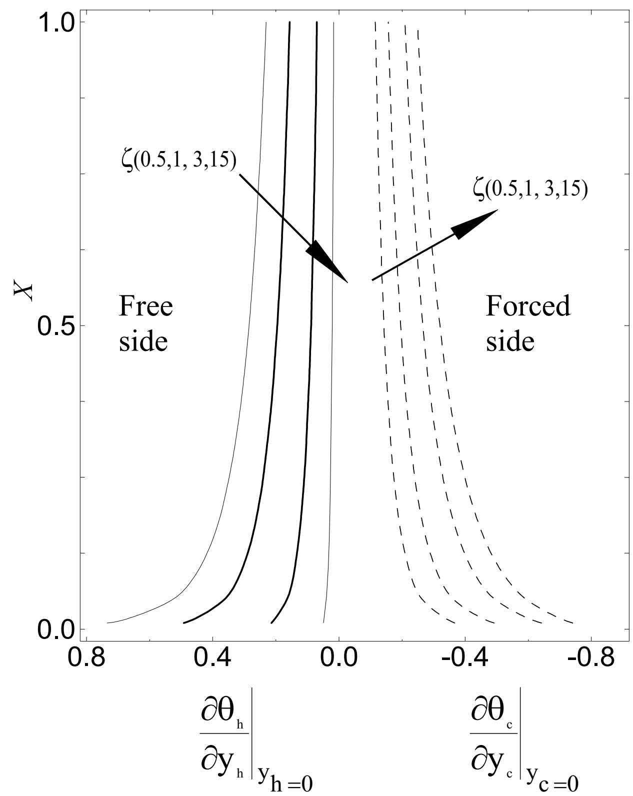


**Figure 5** : Effect of $\zeta$-parameter on fluid temperature gradient at both plate sides, for $Pr_c$=1 and $\omega$=1.

value is very close to –1/2 as $\zeta \to 0$, and very near to 1/2 when $\zeta \to \infty$. However, for more clarity in presentation, the data plotted in Fig. 2 are restricted for: $0.01 \leq \zeta \leq 200$.

Now, our comment on the solution of finite thickness plate case of $\omega > 0$ is reported. Figures 3-11 demonstrate graphically the heat transfer characteristics of this real and more practical case. The variation of two interfacial temperatures $\theta_{wh}$and $\theta_{wc}$ along plate sides with the convection interaction parameter $\zeta$ is displayed in Fig. 3 for $\omega$= 0.2 and $Pr_c$=1. It is noted that for a fixed vertical position $X$, both $\theta_{wh}$and $\theta_{wc}$ rise with the increase in $\zeta$. The effect of $\zeta$-parameter is more clear shown in Fig. 4, where typical temperature profiles across the three regions are plotted at plate mid height ($X$= 0.5) for various $\zeta$ at $Pr_c$=1 and $\omega$= 0.5. These results show that the local interfacial temperature on both sides rises with the increase in $\zeta$-value. The results of Fig. 5 indicate that for a higher value of $\zeta$, the local fluid temperature gradient at wall surface assumes a higher value on the forced convection side and a lower value on the free convection side. This means that the heat transfer effectiveness of the forced convection layer increases while that of the free layer decreases with increasing$\zeta$. This explains the physical significant of $\zeta$-parameter defined by Eq. (25).

The influence of $\omega$-parameter on the interfacial temperature at both sides is shown in Fig. 6. It is clear that at a fixed vertical position, increasing $\omega$ decreases $\theta_{wc}$ while increases$\theta_{wh}$. This means that the temperature drop across the plate increases with $\omega$ due to the increase in the thermal resistance of the plate that acts as a thermal insulator between the two fluid media. The data plotted in Fig. 7 show that for a higher $\omega$-value, the local fluid temperature gradient at both plate sides assumes a lower value over the entire height. It is also noted that for a fixed $\omega$-value, this gradient assumes a max. value at the start point of boundary layer on both sides, which decreases with altitude due to the development of layer thickness (cf., Fig. 8).

The effect of Prandtl number $Pr_c$ of the cold fluid on the thickness of convection layer on both sides is presented in Fig. 8. It is clear that for higher $Pr_c$, the thickness

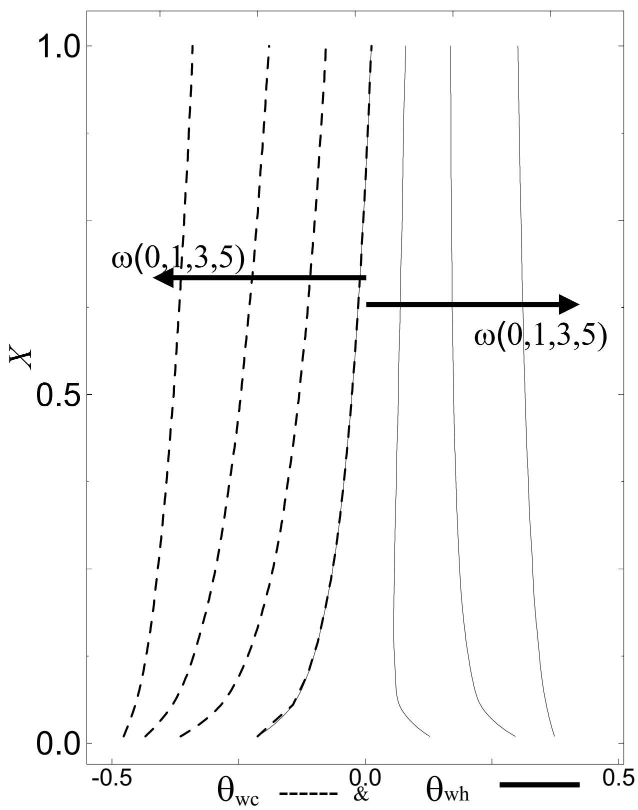


**Figure 6** : Effect of ω-parameter on interfacial temperature at both plate sides, for $Pr_c$=1 and ζ=1.

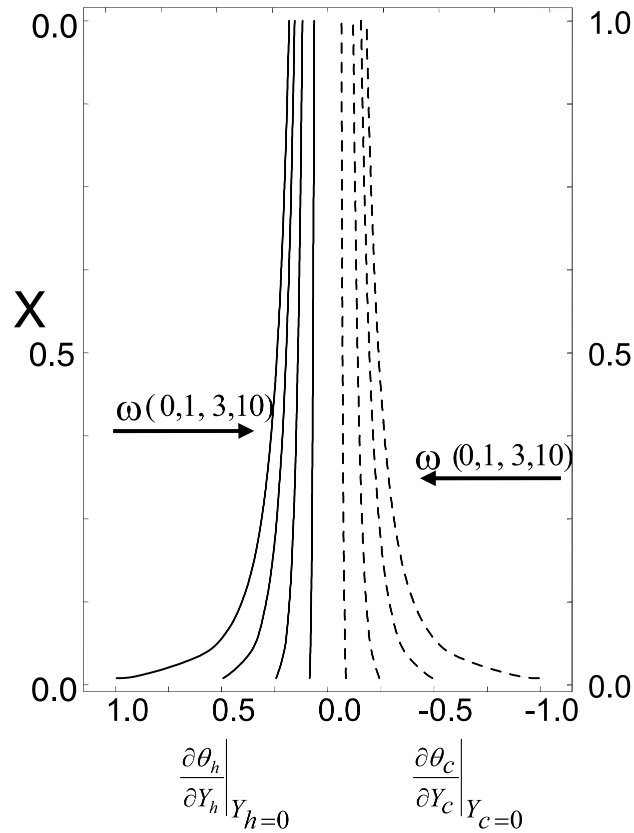


**Figure 7** : Effect of ω-parameter on fluid temperature-gradient at both plate sides, for $Pr_c$=1 and ζ=1.

of forced convection layer is thinner, while no significant effect on the thickness of free layer is noted.

Numerical data obtained for the local Nusselt number of forced convection side $Nu_{xc}$,calculated by Eq. (32), are displayed in Fig. 9 for various values of ω. These data are bounded by the two known exact solutions of forced convection on surfaces with uniform temperature and uniform heat flux. It is noted that the numerical solution approaches the exact uniform heat flux solution as ω increases. A similar conclusion can be made on the effect of ω-parameter on the local Nusselt number of free convection side $Nu_{xh}$,calculated by Eq. (31). However, the results of this case are not presented in the interest of space as well as to avoid repetition.

The dependence of the local Nusselt number of the free convection side $Nu_{xh}$ on the Prandtl number $Pr_c$ of the forced–flowing cold fluid is shown in the lower part of Fig. (10). It is clear that $Pr_c$ has a negligible effect. However, this is not the fact for the effect of $Pr_c$ on the local Nusselt number of the forced convection side $Nu_{xc}$, shown in the upper part of Fig. 10, where this effect could be well correlated by introducing the factor $Pr_c^{1/3}$. The results plotted in Fig. 8 confirm those of Fig. (10).

Numerically obtained values of mean conjugate Nusselt number $\overline{Nu}$, defined by Eq. (34), are displayed in Fig. (11) as a function of ω- and ζ-parameters. It is clear that the first upper curve of ω=0, is bounded by the two asymptotic lines of two exact results (37) & (38) of free and forced convection on vertical isothermal surfaces. This result of ω =0 is the same one of our previous simple model, in which the separating wall was assumed as a partition of zero thermal resistance. This again proves the validity of present approach. In general, the results of Fig. 11 show that the mean conjugate Nusselt number increases with ζ and decreases with ω.

Using a data fitting process, numerical values of mean conjugate Nusselt number, obtained for $0 \le \omega \le 5$ *and* $0 \le \zeta \le 100$, could be correlated within ± 9.2 %

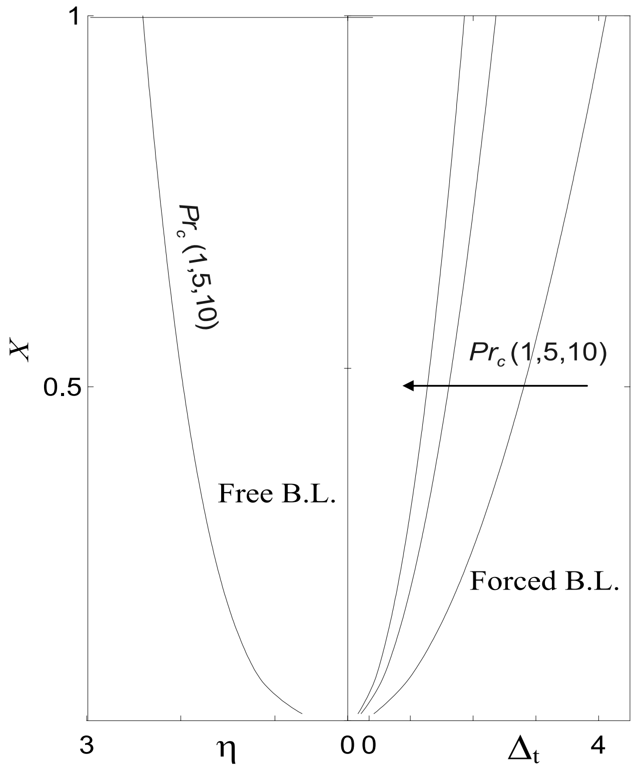


**Figure 8** : Effect of cold-fluid Prandtl number $Pr_c$ on convection layer thickness at both plate sides, for ω=0.5 and ζ=1.

by:

$$\overline{Nu}/(Re^{1/2}Pr^{1/3}) = \left[0.621\zeta e^{-\zeta^{0.531}} + 0.664(1-e^{-0.092\zeta^{0.930}})\right]F(\omega); \tag{39}$$

$$F\omega = 1 - 0.0014\left(1+0.267\omega^{0.15}\zeta^{0.1}\right)^{20.743}; \quad 0 \le \zeta \le 1 \tag{40}$$

$$F(\omega) = 1 - 0.000367\left(1+\frac{0.5\omega^{0.149}\zeta^{0.025}}{(1+\omega^{0.149}\zeta^{0.025})}\right)^{29.923}; \quad 1 < \zeta < 100 \tag{41}$$

For the thin-wall limit, the above correlation reduces to relations (37) & (38) of free and forced convection on isothermal surfaces, for $\zeta \to 0$ and $\zeta \to \infty$, respectively

Comparison of above correlation (39-41) against correlated data (1450 points) is demonstrated in Fig. 12, where every fourth data point was only printed.

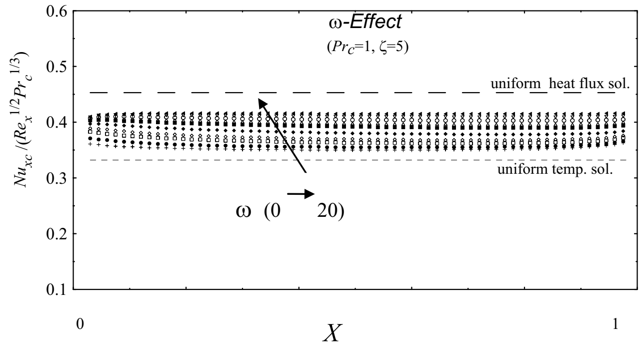


**Figure 9** : Dependence of local Nusselt number of forced convection side on ω.

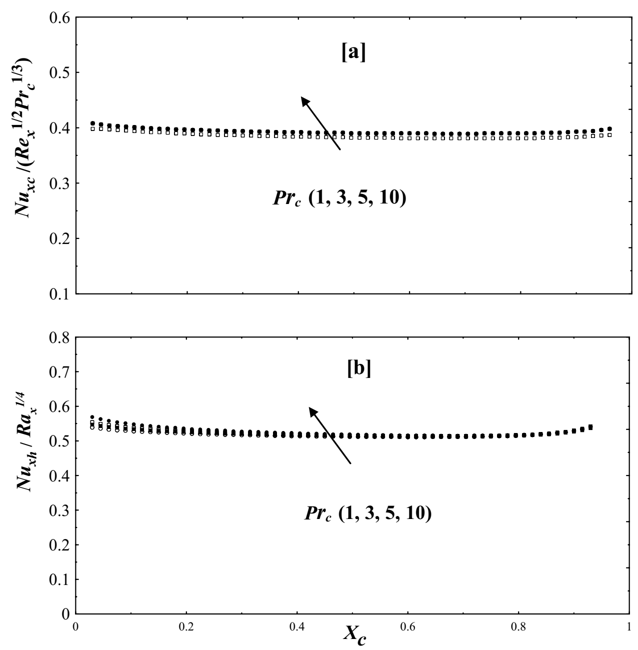


**Figure 10** : Effect of Prandtl number of cold fluid $Pr_c$ on local Nusselt number of (a) forced convection side (b) free convection side.

## 4 Fluent Test

So far, it has been proven that for the thin-wall limit of ω = 0, the present model validates our previous simple model of negligible wall resistance. Furthermore, it yields, as special solutions, the well-known relations (37) & (38) of free and forced convection on isothermal surfaces. However, there is no another relevant work available in literatures (to authors' knowledge) that can be used to do comparison with to do further tests on present model validity. Therefore, a special model problem has

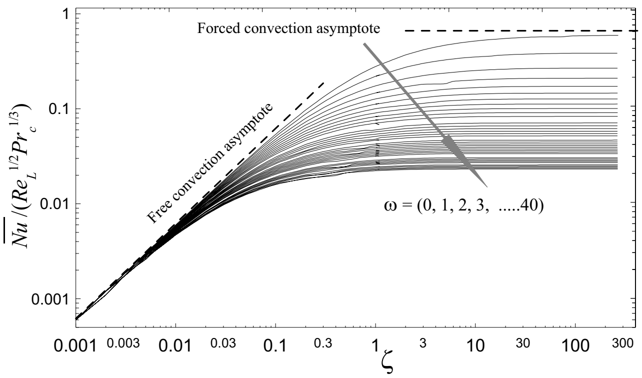


**Figure 11** : Mean conjugate Nusselt number as a function of ζ- and ω-parameters.

been constructed and solved numerically by Computer Code Fluent V 4.4. This numerical software was used by some authors (e.g., Chen (2002) among others) for solving similar conjugate problems. With reference to Fig. 1, the boundary data as well as solid and fluid parameters used in constructing this problem are: Standard oil engine at $T_{h\infty}$= 100$^o$C as the hot fluid, water with $T_{c\infty}$= 60$^o$C and $u_\infty$= 0.1 m/s as the cold fluid, and steel slab ($L$=0.3, $b$= 2 mm or 5 *mm*, $k$ =*14* $W.m^{-2}.K^{-1}$ ) as the separating wall. The thin and thick plates were chosen from the same material in order to highlight the effect of longitudinal heat conduction that was neglected in the analytical model. The comparison between Fluent and model results for the two cases are presented in Figs. (13) and (14). For the case of thin-plate ($b$=2 *mm*, ω=0.09, ζ= 0.18), the comparison (cf., Fig. 13) indicates well agreement between the two solutions with a mean relative deviation of less than 2%. However, for the thick plate case ($b$= 5 *mm*, ω = 0.23, ζ= 0.18), the comparison (cf., Fig. 14) shows a considerable difference between the two solutions, especially over the start region of two convection layers, where the longitudinal variation in the slab temperature is relatively significant. Therefore, the discrepancy between the two solutions may be attributed to the longitudinal heat conduction effect that was neglected in the analytical model.

As a brief conclusion for the Fluent solution, the equations governing mass, momentum and energy in the two convection layers were solved numerically, under the same boundary layer conditions and simplifications adopted in the analytical model, by using a control volume discretization procedure. A second order upwind formula was used for the discretization of energy and momentum equations. The body force weighted scheme was used as the pressure interpolation scheme. A SIMPLEC algorithm was used as the method for pressure-velocity coupling. A segregated solver was employed for simultaneous solution of discretized equations. Under-relaxation factors were employed to control the solution convergence. The adopted convergence criterion was a variation of less than $10^{-7}$ in temperature, and less than $10^{-6}$ in velocity over all grid points. A quadrilateral cell with successive ratio of 1.02 was decided for all edges throughout the fluid domain, whereas equally spaced nodes were used in the solid slab. The numerical solution was validated with the known exact solutions of laminar free and forced convection on isothermal vertical surfaces.

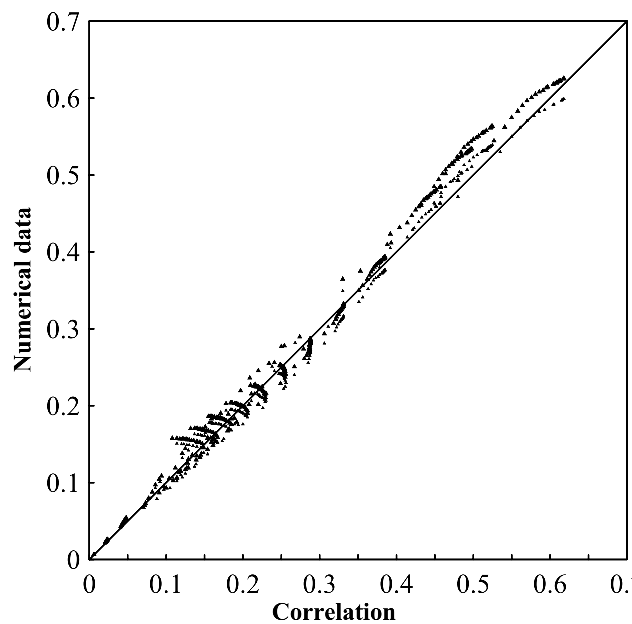


**Figure 12** : Correlation (39) against correlated numerical data.

## 5 Conclusions

Coupled heat transfer between two parallel-flow boundary layers of free and forced convection on vertical plate sides has been analyzed by considering the heat conduction across the plate. The free convection layer was analyzed by the Oseen technique, while the forced layer was treated by the integral technique. The main points that can be summarized from this work are:

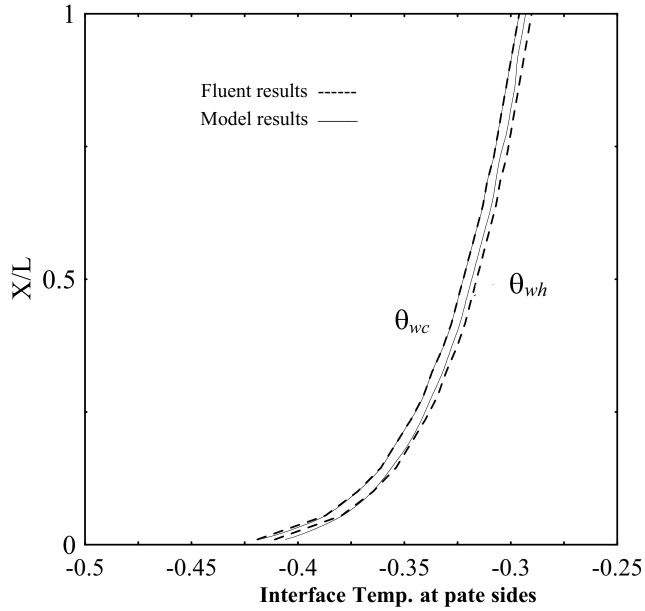


**Figure 13** : Comparison of model predictions with Fluent results for thin-plate case (b= 2 mm, ω = 0.09, ζ= 0.18)

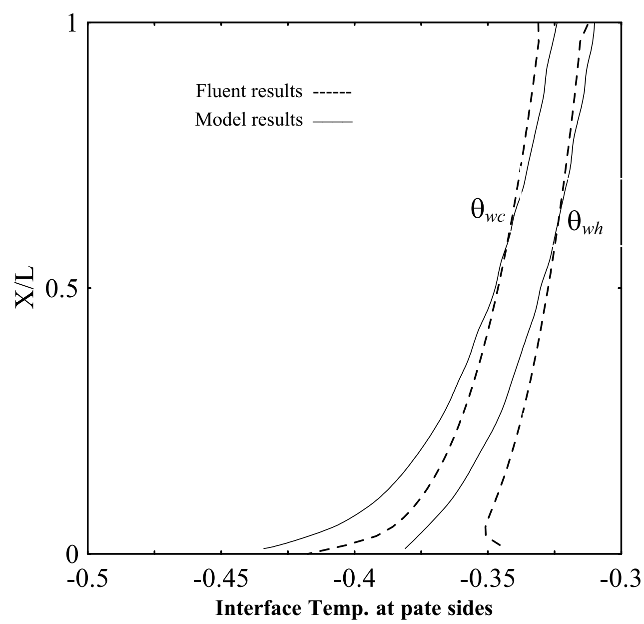


**Figure 14** : Comparison of model predictions with Fluent Results for thick plate case (b= 5 mm, ω = 0.23, ζ= 0.18)

1. Thermal communication between two convection layers is mainly controlled by two dimensionless parameters: ω values the thermal resistance of solid plate to forced layer resistance, and ζ relates the thermal resistance of free layer to forced layer.
2. Present model verifies a previous simple model of negligible wall thermal resistance
3. As special solutions, the model yields the known relations of free and forced convection on isothermal vertical surfaces.
4. Interfacial temperature on both plate sides rises with ζ-value.
5. Temperature drop across the plate rises with ω-value
6. Comparison between model predictions and Fluent results indicates a reasonable agreement at low values of ω-parameter.
7. An implicit expression has been found by means of data-fit procedure for calculating mean conjugate Nusselt number as a function of ω and ζ parameters. This number increases with ζ while decreases with ω.

## References

**Anderson, R., Bejan, A. (1980):** Natural convection on both sides of a vertical wall separating fluids at different temperatures*: Int . J. Heat Transfer*, vol. 102, pp. 630-635.

**Baehr, H.D., Stephan, K. (1998):** Heat and Mass Transfer; Springer, Berlin.

**Bejan, A., Anderson, R. (1981):** Heat transfer across a vertical impermeable partition imbedded in porous medium: Int. J. Heat and Mass Transfer, vol. 24, pp. 1237-1245.

**Bejan, A., Anderson, R. (1983):** Natural convection at the interface between a vertical porous layer and an open space: *Int . J. Heat Transfer*, vol. 105, pp. 124-120.

**Chen, X., Han, P**. (2002): A note on the solution of conjugate heat transfer problem using simple-Like algorithms: *Int. J. Heat and Fluid Flow*, vol. 21, pp. 463-467.

**Gill, A.E.** (1966): The boundary-layer regime for convection in a rectangular cavity: *J. Fluid Mechanics*, vol. 26, pp.515-536.

**Lock, G.S.H., Ko, R.S**. (1973): Coupling through a wall between two free convection systems*: Int. J. Heat Mass Transfer*, vol. 16, pp. 2087-2096.

**Mori, S., Kataya, M., Tanimoto, A**. (1980): Performance of counter flow, parallel plate heat exchangers under laminar flow conditions: *J. Heat Mass Transfer Engng*, vol. 2, pp. 28-38.

**Mosaad M; Al-Hajeri; M**. (2006): Thermal interaction between two vertical systems of free and forced convection: *J. Thermophysics and Heat Transfer* (AIAAJ), vol. 20, no. 2, pp. 305-312.

**Mosaad M; Ben-Nakhi A**. (2003): Conjugate parallel-flowing free and forced convection boundary layers on vertical wall sides of negligible resistance: *Int. J. Heat and Mass Transfer* (Springer Verlag), vol. 39, pp. 177-182.

**Mosaad, M**. (1999): Natural convection in a porous medium coupled across an impermeable vertical wall with film condensation: *J. Heat and Mass Transfer* (Springer Verlag), vol. 35, pp 177-183.

**Poulikakos, D**. (1986): Interaction between film condensation on one side of a vertical wall and natural convection on the other side: *Int. J. Heat Transfer*, vol. 108, pp. 560-566.

**Sakakibara, M., Amaya, H.** (1992): Conjugate heat transfer between two vertical natural convection reservoirs separated by a vertical plate*: Int. J. Heat and Mass Transfer*, vol. 35, pp. 2289-2297.

**Sparrow, E.M., Faghri, M.** (1980): Fluid-to-fluid conjugate heat transfer for a vertical pipe-internal forced convection and external natural convection*: Int. J. Heat Transfer*, vol. 102, pp. 402-407.

**Sparrow, E.M., Gregg, J.L**. (1965): Laminar free convection for a vertical surface with uniform surface heat flux: *Trans. ASME*, vol. 78, pp. 435-440.

**Trevino, C., Mendezc, F., Higuera, F.G.** (1996): Heat transfer across a vertical wall separating two fluids at different temperatures*: Int. J. Heat and Mass Transfer*, vol. 39, pp. 2231-2241.

**Vaszi, A. Z., . Ingham, D. B., Lesnic, D., Munslow, D., PoP, I.** (2001): Conjugate Free Convection from Slightly Inclined Plate embedded in a Porous Medium: *J. ZAMM*, vol. 81, pp..465 – 479.

**Viskanta, R., Lankford, D.W**. (1981): Coupling of heat transfer between two natural convection systems separated by a vertical wall*: Int. J. Heat Mass Transfer*, vol. 24, pp. 1171-1177.

**Appendix A:**

For $\theta_{wh}$= -1/2 in Eqs. (16) & (17), one gets, respectively,

$$\left.\frac{\partial\theta_h}{\partial Y_h}\right|_{Y_h=0} = \lambda, \tag{42}$$

$$\lambda = \left(\frac{3}{64X}\right)^{1/4}. \tag{43}$$

Substituting Eqs. (42) & (43) into Eq. (35) yields

$$\frac{\overline{Nu}}{Ra^{1/4}} = \int_0^1 \lambda dX = \int_0^1 \left(\frac{3}{64X}\right)^{1/4} dX = 0.621 \tag{44}$$

The above result is the same one of laminar free convection on an isothermal vertical surface, obtained by a similarity solution for $\mathrm{Pr}_h >>1$.

**Appendix B:**

For $\theta_{wc}$= +1/2 in Eqs. (6) & (8), one gets, respectively,

$$\left.\frac{\partial\theta_c}{\partial Y_c}\right|_{Yc=0} = -\frac{3}{2\Delta_t}, \tag{45}$$

$$\Delta_t = 0.9756 Pr_c^{-1/3}\left(\frac{280}{13}X\right)^{1/2}. \tag{46}$$

Substituting Eqs. (46) & (47) into Eq. (33) yields

$$\frac{\overline{Nu}}{Re^{1/2}Pr_c^{1/3}} = \frac{-1}{Pr_c^{1/3}}\int_0^1 -\frac{3}{2\Delta_t}dX$$

$$= \int_0^1 \frac{3/2}{0.9756\left(\frac{280}{13}X\right)^{1/2}}dX = 0.664 \tag{47}$$

This result is the same known similarity solution of forced convection on an isothermal surface.